THE SURFACE DENSITY OF HALOES

A. Del Popolo[1,2,3,4] and Xi-Guo Lee[4]

[1] *Dipartimento di Fisica e Astronomia, Universitá di Catania, Viale Andrea Doria 6, 95125 Catania, Italy*

[2] *INFN, sezione di Catania, Via Santa Sofia 64, 95123 Catania, Italy*

[3] *International Institute of Physics, Universidade Federal do Rio Grande do Norte, 59012-970 Natal, Brazil*

[4] *Institute of Modern Physics, Chinese Academy of Sciences, Post Office Box 31, Lanzhou 730000, Peoples Republic of China*

Abstract. We study the correlation between the central surface density and the core radius of the dark matter haloes of galaxies and clusters of galaxies. We find that the surface density within the halo characteristic radius r_* is not a universal quantity as claimed by some authors (e.g., Milgrom 2009), but it correlates with several physical quantities (e.g., the halo mass M_{200}, and the magnitude M_B). The slope of the surface density-mass relation is 0.18 ± 0.05, leaving small room to the possibility of a constant surface density. Finally, we compare the results with MOND predictions.

Key words: cosmology: theory – large-scale structure of universe – galaxies: formation

1. INTRODUCTION

According to recent releases of the Planck observatory, our universe is characterized by the matter density parameter $\Omega_m = 0.315 \pm 0.017$ (Ade et al. 2014)[1], and the physical densities of baryons and dark matter (DM), $\Omega_b h^2 = 0.02205 \pm 0.00028$ and $\Omega_c h^2 = 0.1199 \pm 0.0027$, respectively. The rest of mass is in the form of dark energy ($\Omega_\Lambda = 0.685$).

The model which better describes the physical features of our Universe at intermediate and large scales is the ΛCDM model, in which the Universe is constituted of the above quoted constituents (Del Popolo 2007, 2013, 2014a). Despite the self-consistency and remarkable success of this model, some problems are still on the table.

One area of active investigation is testing predictions of the ΛCDM model at scales from a few kpc to tens of pc (i.e., the smallest scales probed by observations of galaxies). An example is the fact that substructures, such as small haloes and

---

[1] In the 2015 Planck's release, $\Omega_m = 0.308 \pm 0.012$.

galaxies orbiting within larger units, may not be as common as is expected on the basis of numerical simulations of cold collisionless dark matter. This problem has been dubbed the "missing satellites problem", to whom is related the too-big-to-fail problem (Klypin et al. 1999; Del Popolo & Gambera 1997; Del Popolo et al. 2014; Del Popolo & Le Delliou 2014). Another problem is the determination of the total mass of virialized haloes (Del Popolo & Gambera 1996; Del Popolo 2002; Hiotelis & Del Popolo 2006, 2013) (galaxy and galaxy clusters), and their density profiles. As regards the issue of density profiles, there is a tension between ΛCDM predictions and observations of the central dark matter distribution in galaxies (Moore 1994; Cardone & Del Popolo 2012 (CD12); Del Popolo et al. 2013a; Saburova & Del Popolo 2014 (SD14); Del Popolo & Hiotelis 2014).

Notably, the tensions quoted have not gone away during the past 10–15 years, even though both theoretical models and observations have improved dramatically. On larger scales the cosmological constant problem (Weinberg 1989; Astashenok & Del Popolo 2012), and the cosmic coincidence problem, afflict the model.

Finding the origin of some of such discrepancies is complicated mainly due to the lack of understanding of the complex hydrodynamical phenomena in hot dense plasma. A valuable help to address this problem comes from the scaling relations between DM halo parameters and stellar quantities.

In this context, Kormendy & Freeman (2004) found several interesting relations among DM halo parameters, obtained through mass modeling of the rotation curves of 55 galaxies using a pseudo-isothermal profile as a fitting profile. An intriguing property that they found is that the quantity $\mu_{0D} = \rho_0 r_0 \simeq 100 M_\odot/\mathrm{pc}^{-2}$ (see note[2]), proportional to the halo central surface density for any cored halo distributions, is nearly independent of the galaxy's blue magnitude. The validity of this relation has been much debated in the literature (Donato et al. 2009 (D09); Gentile et al. 2009 (G09); Boyarsky et al. 2009 (B09); Cardone & Tortora 2010 (CT10); Napolitano, Romanowsky & Tortora 2010 (NRT10); CD12; SD14).

D09 repeated the analysis by Kormendy & Freeman (2004, hereafter KF04) by means of rotation curves of $\simeq 1000$ spiral galaxies, the mass models of individual dwarf and spiral galaxies and the weak lensing signal of elliptical and spirals and found strong evidence for the constancy of the central DM column density, over 12 orders of magnitude in luminosity. They found $\log \mu_{0D} = 2.15 \pm 0.2$, in units of $\log(M_\odot/\mathrm{pc}^2)$.

Prompted by the previous claim, Milgrom (2009) showed that modified Newtonian dynamics (MOND) predicts, in the Newtonian regime, a quasi-universal value of μ_{0D} for every different kind of internal structure and for all masses.

Opposite results were obtained by B09, NRT10, CT10, CD12, and SD14 that show a systematic increase in surface density with luminosity L_V, the stellar mass M_*, the halo mass M_{200}, morphological type, $(B - V)_0$ color index, and content of neutral hydrogen.

NRT10 showed that, within effective radius, the projected density of local early type galaxies (ETGs) is, on average, systematically higher than the same quantity for spiral and dwarf galaxies, pointing to its systematic increase with halo mass as suggested by B09. B09 extended the above analyzed samples to both group and cluster scale systems and found that the dark matter column density, S, (defined

---

[2] ρ_0 and r_0 are, respectively, the central density and core radius of the adopted pseudo-isothermal cored dark matter density profile.

in the following and equivalent to μ_{0D} in the case of fitting with a Burkert profile) is given by

$$\log S = 0.21 \log \frac{M_{\text{halo}}}{10^{10} M_\odot} + 1.79 , \qquad (1)$$

with S in $M_\odot/\text{pc}^2$.

CT10, by modeling the dark halo with a Navarro - Frenk - White profile (NFW) and assuming a Salpeter initial mass function (IMF) to estimate stellar masses, found that the column density and the Newtonian acceleration within the halo characteristic radius r_s and effective radius R_{eff} are not universal quantities, but correlate with the luminosity L_V, the stellar mass M_* and the halo mass M_{200}.

In order to try to discriminate among these results and to find an explanation and analytical derivation of the surface density of haloes, we analyze the problem using the secondary infall model (SIM) introduced in Del Popolo & Kroupa (2009) (DPK09), taking into account ordered and random angular momentum, dynamical friction, and baryon adiabatic contraction.

The paper is organized as follows: in Section 2, we discuss how surface density was obtained by different authors, and compare the previous results with the result of our theoretical model. In Section 3, we discuss the implication of the previous results on MOND's prediction. Section 4 is devoted to conclusions.

2. SURFACE DENSITY

The results discussed in the introduction that claim a constancy of the surface density (KF04, D09) of DM and those that claim a mass dependence (e.g., B09, CT10, NRT10, CD12) are fundamentally based on fitting of observed properties of DM haloes.

With the exception of Boyarsky et al. (2010, hereafter B10), no qualitative explanation and/or analytical derivation of the quoted results has been proposed so far. B10 showed, with a very simple and minimal SIM, how the mass dependence of the *dark matter column density*, S, (defined in the following and equivalent to μ_{0D} in the case of fitting with a Burkert profile) is given by $\mathcal{S}(r_s) \propto M^{1/3}$, or $\mathcal{S}(r_s) \propto M^{0.23}$, taking account of deviations from self-similarity.

This relation, in agreement with the simulations of B09, showing a similar trend with mass but with a smaller slope $(\mathcal{S}(r_s) \propto M^{0.21})$, was considered by them as a sort of universal scaling in the DM haloes, insensitive to baryons presence and to the details of DM density distributions. This last result is in contradiction to D09 results because B09 got a universal non-constant surface density, contrarily to D09 who got a universal constant surface density. Therefore, while D09 claimed that the surface density, which is also related to Newtonian acceleration inside the system, is a further proof of the correctness of the Modified Newtonian Dynamics (MOND)(see also Milgrom 2009), B09 and B10 reached the opposite result.

In what follows, we study the mass dependence of the surface density through a much more improved SIM which not only takes into account angular momentum, but also baryons dynamical friction, and adiabatic contraction. The model for determining the density profiles of haloes that will be used to calculate the surface density of haloes has been described in DPK09. The surface density of DM is calculated, starting from the density profiles, as described in the following.

2.1. The S-M relation

As mentioned at the beginning of this chapter, the results claiming a constancy of the surface density (KF04, D09) of DM and those claiming a mass dependence (e.g., B09, CT10) are fundamentally based on fitting of observed properties of DM haloes. KF04 and D09 assumed that all galaxies, from dwarfs to giants ($-5 < M_B < -25$), have a cored density profile. KF04 assumed a pseudo-isothermal profile, and D09 a Burkert profile:

$$\rho(r)_{\mathrm{B}} = \frac{\rho_0 r_0^3}{(r + r_0)(r^2 + r_0^2)}\,.\tag{2}$$

The fit to the rotation curves yields the values of the two structural DM parameters (i.e., r_0 and ρ_0), then the surface density is calculated as $\mu_{0\mathrm{D}} = \rho_0 r_0$.

The previous approach has a strong limits. It is based on the assumption that all the galaxies studied, namely dwarf, spiral and elliptical galaxies, can be fitted by cored models, and the inner slope of the density profile is independent from the halo mass.[3]

In the case of dwarf galaxies, a large part of the studies indicate that the inner part of density profiles is characterized by a core-like structure (e.g., Moore 1994; Kuzio de Naray et al. 2008; Oh et al. 2010, 2011), but some studies found that density profiles are compatible with cuspy and cored profiles (e.g., Hayashi et al. 2004; de Blok et al. 2008). In other terms, while a large part of dwarfs are well fitted by core-like profiles, some of them are not (see also Del Popolo 2012a,b).

In the case of ellipticals, the situation is even more complicated. Several studies (e.g., Mamon & Lokas 2005) showed that the DM profile of ellipticals is cuspy. NRT10 found that early-type-galaxies (ETG) violate the constant density scenario for the other galaxies by a factor of $\simeq 10$ on average, and a factor of $\simeq 5$ in the same mass regime, in agreement with B09.

The quoted discussion implies that when we study the surface density it is preferable to have a method that is able to fit not only cored density profiles but also cuspy or intermediate ones among the two types.

Another more general way of determining the surface density, in the case one uses more than one model density profile for the fit, or in the case the density profile is not a standard one, like the Burkert, NFW, and pseudo-isothermal (ISO) profiles, is to introduce a *dark matter column density*, averaged over the central part of an object:

$$S = \frac{2}{r_\star^2} \int_0^{r_\star} r dr \int dz \rho_{\mathrm{DM}}(\sqrt{r^2 + z^2})\,.\tag{3}$$

The integral over z extends to the virial boundary of a DM halo. The definition (3) implies that S is proportional to the dark matter surface density within $r_\star$ ($S \propto \rho_\star r_\star$)[4]. The quantity S is more general, as it is defined for any (not necessarily cored) DM profile.

---

[3] Several papers showed that the density profile is not universal, and how the inner slope of density profiles depends on mass (Del Popolo 2010, 2011; Babyk et al. 2014; Del Popolo 2014b).

[4] Parameters of different profiles that fit the same DM density distribution are related (for example, r_s for NFW is equal to $6.1r_c$ for ISO profile and equals to $1.6r_{\mathrm{B}}$ for Burkert). Choosing these values as $r_\star$ in each case, one finds that the value of S for NFW and ISO differs by less than 10% (the difference in S between NFW and Burkert is $\sim 2\%$).
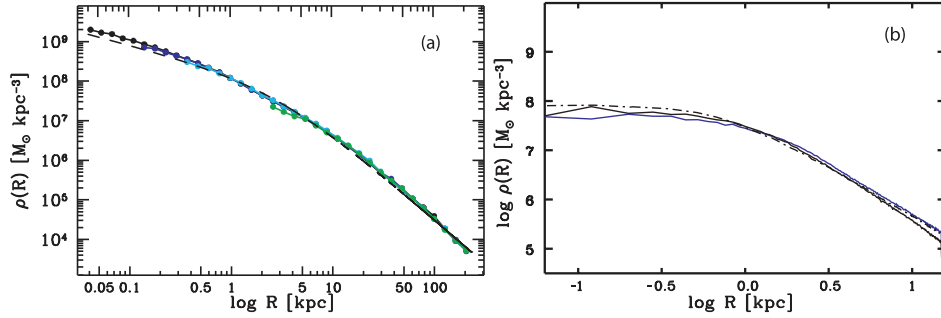
Fig. 1. Comparison of the dark matter density profile of our model with simulations. Panel (a) plots the result of Stadel et al. (2009) dissipationless simulations (solid line), and that of our model (dashed line). Panel (b) plots the result of our model (dot-dashed line) and galaxy DG1 (solid blue line) and galaxy DG2 (solid black line) of Governato et al. (2010) SPH simulations.

In other terms, if the profile is cored, using S we will obtain the same result for the surface density of the Burkert's fit, while in the case the profile is not cored, S will give a more precise value for the surface density than that using the Burkert's model fit (see the following).

The previous method was used by B09, who extended the analysis of D09 to galaxies and galaxy clusters and fitted the DM profiles by means of three different DM profile models, namely the Burkert profile (Eq. 2), the pseudo-isothermal profile (ISO)

$$\rho(r)_{\rm ISO} = \frac{\rho_{\rm c}}{1 + r^2/r_{\rm c}^2} \, , \tag{4}$$

where $r_{\rm c}$ is the ISO core radius, and NFW profile

$$\rho(r)_{\rm NFW} = \frac{\rho_s r_s}{r(1 + r/r_s)^2} \, , \tag{5}$$

where r_s is the typical NFW characteristic radius. CT10 used two DM profiles for the fit, namely the Burkert and ISO profiles.

In order to determine S, we use Eq. (3) together with the density profiles obtained with the model given in Appendix. Before calculating S, we show some examples of the density profiles obtained with the quoted model and a comparison with N-body simulations.

In Fig. 1, we plot the profiles obtained with our model and those predicted by numerical simulations. Fig. 1a shows the result of Stadel et al. (2009) dissipationless simulations (solid line), and that of our model (dashed line). In order to make this comparison, our halo, similarly to that of Stadel et al. (2009), is constituted only by DM. Fig. 1b shows the result of our model (dot-dashed line) and the two galaxies obtained by Governato et al. (2010) SPH simulations, namely their galaxy DG1 (solid blue line) and galaxy DG2 (solid black line). Both Fig. 1a and Fig. 1b show a good agreement between the results of our model and those of simulations.

With the density profile obtained with our model and using Eq. (3) we determine S. The maximum likelihood fit for the correlation $\log \mathcal{S}(r_s)$-$\log M_{200}$ in our

model is

$$\log \mathcal{S}(r_s) = \begin{cases} 0.18 \log\left(\frac{M_{200}}{10^{10} M_\odot}\right) + 1.9, & M_{200} \geq 5 \times 10^{10} M_\odot \\ 2.09, & M_{200} \lesssim 5 \times 10^{10} M_\odot, \end{cases} \tag{6}$$

while CT10 found

$$\log \mathcal{S}(r_s) = 0.16 \log\left(\frac{M_{200}}{10^{12} M_\odot}\right) + 2.11 .^5 \tag{7}$$

Similarly, B09 found

$$\mathcal{S}(r_s) \simeq 0.21 \log\left(\frac{M_{200}}{10^{10} M_\odot}\right) + 1.79, \tag{8}$$

and B10 give $\mathcal{S}(r_s) \propto M^{1/3}$, or $\mathcal{S}(r_s) \propto M^{0.23}$, when taking account of deviations from self-similarity.

The best fit concerning DM haloes in CT10 is shallower than that of B09 and the result of the present paper, although the slope is consistent with B09 (0.21) and the present paper within their large error bars. One has to recall that while CT10 did explicitly take into account the correlated errors on $S(r_s)$ and M_{200}, it is not known if B09 did the same. Then, the difference in slope is only the outcome of the use of different algorithms on noisy data

Fig. 2 shows $\mathcal{S}(r_s)$ for the model of the present paper (long dash - short dash line), B09 (short-dashed line), and B10 (dot-dashed line). The plot shows that $\mathcal{S}(r_s)$ depends on M_{200}. The result of B09 and those of the present paper are similar except at $M_{200} \lesssim 5 \times 10^{10} M_\odot$, where our model predicts a flattening of $\mathcal{S}(r_s)$. The difference at this mass scale is due to the fact that our model is taking account of baryons while that of B09 just DM. The result of B10, based on a much simpler SIM than that used in this paper, gives just a qualitative agreement with other results.

2.2. Comparison of theory and observation of the surface density

In order to compare our results to those of D09 and SD14, we need to find a way to express our result in terms of $\mu_{0D} = \rho_0 r_0$.

In the following, we show some examples for known profiles. Let us first write the $S(r)$ for them. For the pseudo-isothermal profile one obtains:

$$S_{\mathrm{ISO}}(R) = \frac{2\pi \rho_c r_c^2}{R^2}\left[\sqrt{R^2 + r_c^2} - r_c\right]. \tag{9}$$

For the NFW density distribution, we have

$$S_{\mathrm{NFW}}(R) = \frac{4\rho_s r_s^3}{R^2}\left[\frac{\arctan\sqrt{R^2/r_s^2 - 1}}{\sqrt{R^2/r_s^2 - 1}} + \log\left(\frac{R}{2r_s}\right)\right]. \tag{10}$$

---

[5] The marginalized constraints on the scaling relation parameters for the correlation involving $\log \mathcal{S}(r_s)$ and $\log M_{200}$ in our model is $0.18^{+0.05}_{-0.05}$, while in the case of CT10, assuming a fiducial NFW+Salpeter model, is $0.14^{+0.15}_{-0.15}$.
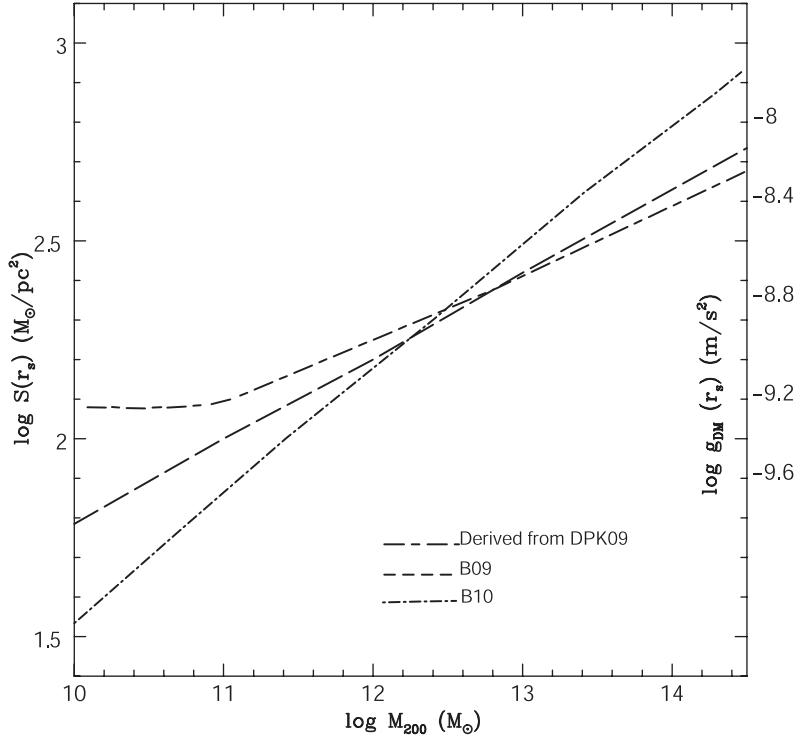
Fig. 2. $\mathcal{S}(r_s)$ as a function halo mass M_{200}. The long dash - short dash line, dashed line, and the dot-dashed line represent $\mathcal{S}(r_s)$ for the model of this paper, B09, and B10, respectively.

An analytical relation between the parameters of several profiles can be obtained fitting the same rotation curve (B09, CT10). For an ISO and NFW profile, one can take an ISO profile, calculates the relative rotation curve and fits the result with a NFW profile. One finds: $r_s \simeq 6.1 r_c$, $\rho_s \simeq 0.11 r_c$. Comparing the column densities for NFW and ISO profiles, whose parameters are related through the relations now written, one obtains:

$$\frac{S_{\mathrm{NFW}}(r_s)}{S_{\mathrm{ISO}}(6r_c)} \approx 0.91 \,. \tag{11}$$

Similarly, for the Burkert profile and NFW: $r_s \simeq 1.6 r_0$, $\rho_s \simeq 0.37 \rho_0$ and

$$\frac{S_{\mathrm{NFW}}(r_s)}{S_{\mathrm{Burkert}}(1.6 r_0)} \approx 0.98 \,. \tag{12}$$

The difference between the column densities S_{NFW}, S_{Burkert} and S_{ISO} turns out to be less than 10% (CT10). Then, $S_{\mathrm{NFW}}(r_s) \approx 0.98 \, S_{\mathrm{Burkert}}(1.6 \, r_0) \approx 0.91 \, S_{\mathrm{ISO}}(6 \, r_c) \approx 1.89 \, r_0 \rho_0$.

In Fig. 3, we compare the result of the present model with the D09 and SD14 results. SD14 extended the sample of CD12. The sample consists of 211 galaxies of different types. The complete sample of galaxies with its properties can be found
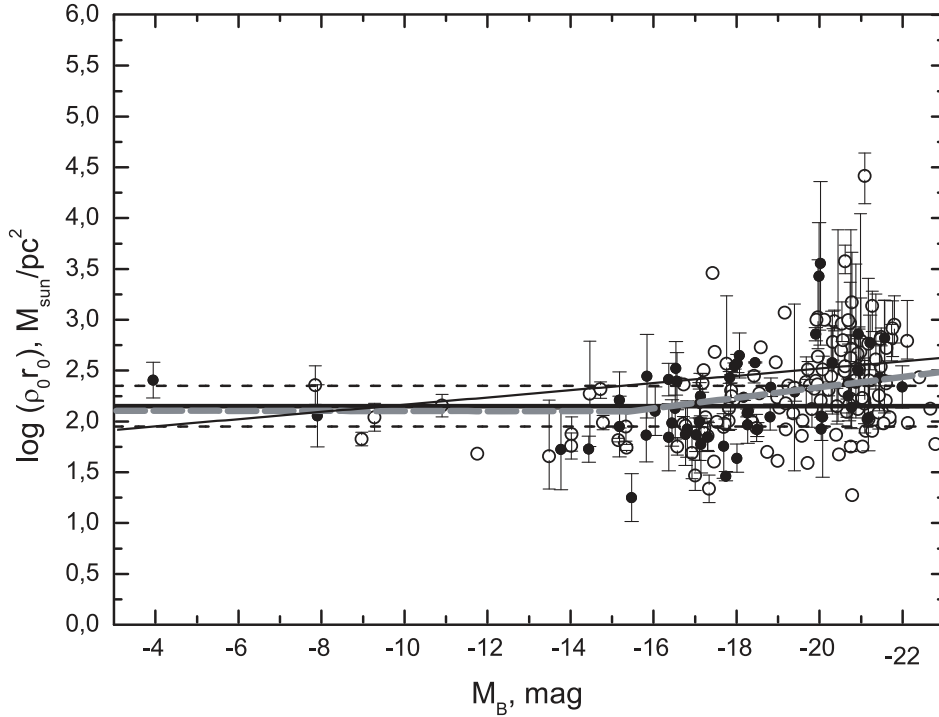
Fig. 3. The quantity $\rho_0 r_0$ in units of $M_\odot/\mathrm{pc}^2$ as a function of galaxy magnitude for different galaxies and Hubble types. See explanation in the text.

online (http://mnras.oxfordjournals.org/content/ suppl/2014/10/30/stu1957.DC1 /table.txt). Since different approaches could lead to different DM parameters, SD14 used DM parameters obtained by different approaches in order to compensate for the uncertainties in each particular approach.

In Fig. 3, the thick-solid and dashed black lines represent the value of $\log \mu_{0\mathrm{D}} = 2.15 \pm 0.2$ obtained by D09. The circles correspond to DM surface densities obtained using the quoted sample and with different methods described in SD14. The filled symbols represent the averaged estimates of $\log \mu_{0\mathrm{D}}$ when a galaxy was present in more than one source. The thin solid line represents the result of our model for the surface density when considering galaxies made of only dark matter. Differently from this case (galaxies constituted of DM only), the dashed light grey line denotes the surface density obtained when taking into account all effects considered in DPK09. For masses lower than $\simeq 5 \times 10^{10} M_\odot$ and magnitudes brighter than $M_B \simeq -14$, the surface density is constant. However, a systematic change of the average column density $\rho_0 r_0$ as a function of the object's mass is clearly present for larger masses, the data being well fitted as $\rho_0 r_0 \propto M^\alpha$ with $\alpha = 0.18 \pm 0.05$. Such results make, therefore, us safely argue against the constancy or universality of the surface density[6] claimed by KF04 and D09.

---

[6] Or $\mathcal{S}_{\mathrm{DM}}$ (i.e., $\mathcal{S}_{\mathrm{DM}} = \mathrm{const}$).

3. IMPLICATIONS FOR MOND

The small scale problems of the ΛCDM model mentioned in the introduction can be solved through two different approaches: (a) "cosmological solutions" and (b) "astrophysical solutions". One of the solutions belonging to the first group is MOND.

In the early 1980s Milgrom (1983a,b), based on the fact that typical accelerations in galactic systems are many orders of magnitude smaller than those encountered in the solar system, proposed a modified dynamics based on the acceleration as the relevant system parameter. This modified dynamics, MOND, introduces a constant with the dimensions of an acceleration, a_0, and posits that standard Newtonian dynamics is a good approximation only for accelerations that are much larger than a_0. More precisely, there are two different "interpretations" of his idea:

(a) modification of Newton's second law of motion, from the usual

$$\mathbf{F} = m\mathbf{a} \tag{13}$$

to

$$\mathbf{F} = m\mu[a/a_0]\mathbf{a}, \tag{14}$$

where $\mu(x)$ is an interpolating function satisfying the conditions

$$\mu[x] = \begin{cases} 1, |x| \gg 1 \\ x, |x| \ll 1 \end{cases}, \tag{15}$$

in other terms, $\mu[a/a_0]$ is a function with value 1 for high values of the acceleration and a/a_0 for small accelerations, and $a_0 \simeq 10^{-10}\mathrm{m/s}^2$ is a universal constant. When a test particle is subject to an acceleration $a \ll a_0$, one has

$$F = GM/r^2 = \mu(a/a_0)a_\mathrm{N} \tag{16}$$

leading to

$$a_\mathrm{N} = \sqrt{GMa_0}/r. \tag{17}$$

Newtonian dynamics holds when $a \gg a_0$.

(b) DM is highly correlated to luminous matter according to a specific law.

Two consequences of Eqs. (16) and (17) are: (1) that orbital speed on a circular orbit, far away from a mass M is independent of radius[7]; (2) this asymptotic rotational speed depends only on the total mass M via $V^4 = GMa_0$. In MOND, this is the fact underlying the observed Tully-Fisher-type relations. Another point in favor of MOND is that the majority of LSB galaxies observed are consistent with the rotational curve predicted by MOND.

Milgrom (2009) showed that MOND predicts, in the Newtonian regime, a quasi-universal value of $\mu_{0\mathrm{D}}$ ($\log \mu_{0\mathrm{D}} = 2.14$) for every different kind of internal structure and for all masses. This value is very close to that obtained by D09, shown in Fig. 3 by a thick black line. According to Milgrom (2009), the quasi-universal value is not shared by objects with low surface densities, so the DM surface density could

---

[7] In reality this is not a consequence of MOND, but a guiding principle used to build up MOND, which took asymptotic flatness of galaxy rotation curves as an axiom.

be lower. Thus, we should expect the DM surface density to be around 2.14 or lower. As can be seen from Fig. 3, this prediction is not confirmed by SD14 data for high-luminosity systems and by the predictions of our model (grey dashed line).

Moreover, in Fig. 3 we show that up to a certain M_B the surface density follows a constant behavior, similar to that predicted by D09, and after that it starts to increase. This means that the surface density is not universal, but depends on magnitude and mass. In summary, our result shows that MOND is working well in the case of dwarf galaxies and spirals, but going further with mass it does not work well. This result is in agreement with what is already known, namely, that MOND has difficulties in reproducing results connected with clusters of galaxies, large scale structure, Cosmic Microwave Background anisotropies, the current accelerated expansion and initial conditions for the Big Bang, gravitational lensing.

For precision's sake, we recall that some papers evidence problems of MOND even in the case of dwarf galaxies and on galactic scales. After a detailed formulation of the dynamical friction problem under the alternative hypothesis of MOND dynamics and in the lack of any dark matter, Sanchez-Salcedo et al. (2006) have shown that due to the enhanced dynamical drag of the stars the dynamical friction timescales in MOND, even in the case of dwarfs, would be extremely short. Ferreras et al. (2008) found that strong gravitational lensing on galactic scales requires a significant amount of dark matter, even within MOND. More recently, Hashim et al. (2014) showed that MOND gives a bad fit to the rotation curve of the galaxy ESO 138-G014. Moffat & Toth (2014) found that MOND predictions do not agree with the Milky Way (MW) rotation curve data. Randriamampandry & Carignan (2014) found that in 15 dwarfs and spirals, a_0 is different from that postulated by MOND. Similarly, Adams et al. 2014 found different values of a_0 for the dwarf galaxies they studied. Iocco, Pato & Bertone (2015) found that the previously discussed interpolating function is unable to describe at the same time the rotation curve of the MW and that of external galaxies.

We finally recall that our result is in agreement with those of B09, NRT10, and CT10, CD12, SD14, converging on the result that the surface density is not constant.

4. CONCLUSIONS

Using the SIM model introduced in DPK09, we study the correlation between the central surface density and the halo core radius of galaxy and cluster of galaxies dark matter haloes. Differently from what claimed KF04, or D09, the column density within the halo characteristic radius r_* is not a universal quantity. The surface density obtained, $S \propto M^{0.18\pm0.05}$, leaves small room to the possibility of a constant surface density, as claimed previously by the quoted authors.

The quoted constancy of surface density and Newtonian acceleration in r_0 is one of MOND's predictions. Rephrasing Milgrom (2009), the surface density is constant for objects of any internal structure and mass, if they are in the Newtonian regime (see Milgrom 2009). This MOND prediction is not confirmed by our result.

The non self-similar behavior of the surface density and acceleration generated by DM shows that while MOND paradigm is finely working for dwarfs and spirals of small mass, it has increasing difficulties with increasing mass.

APPENDIX. MODEL

The results discussed in the introduction, claiming a constancy of the surface density (D09; G09) of DM and those claiming a mass dependence (B09, CT10), are fundamentally based on fitting of observed properties of DM haloes. With the exception of B10, no qualitative explanation and/or analytical derivation of the quoted results has been proposed so far. B10 used a SIM and supposed that the halo density profile evolves in a self-similar way. They arrived at the conclusion that $S \propto M^{1/3}t^{-4/3}$, qualitatively in agreement with B09 simulations and CT10 results, in the sense that S increases with mass, but the slope is much higher than that obtained by B09 and CT10.

The quoted discrepancy could be connected to the oversimplified structure of the SIM used. Even if they tried to use the improved SIM of Sikivie et al. (1997), taking account of angular momentum, these effects on collapse, in reality, are not properly taken into account.

In what follows, we give a brief description of how we implement the SIM approach to get the density profile of the dark matter halo referring the interested reader to DPK09 for further details.

In most popular cosmological scenarios, the density field soon after recombination can be represented by a Gaussian random field. High density contrast peaks in the field will eventually achieve overdensities of order 1 and enter a non-linear stage of evolution. These peaks will then collapse to form bound structures.

A model often used to study the non-linear evolution of perturbations of dark matter is the SIM or standard spherical collapse model (SSCM) introduced by Gunn & Gott (1972) and extended in subsequent papers (Ryden & Gunn 1987; Del Popolo 2009; Cardone et al. 2011a,b; Del Popolo 2012a,b; Del Popolo et al. 2013b,c,d; Pace et al. 2014).

We start with one of these peaks, and, for simplicity, assume that it is spherically symmetric. Following Ryden & Gunn (1987) (RG87), Ryden (1988a,b) (R88a, R88b), and DPK09, the peak is divided into a very small central core and many spherically symmetric concentric mass shells, each labeled by its initial comoving distance from the center, x. A bound mass shell of initial comoving radius x_i expands up to a maximum radius, x_m (or turnaround radius x_{ta}). As successive shells expand, they acquire angular momentum and then contract on orbits determined by the angular momentum itself, while dissipative processes and eventual violent relaxation intervene to virialize the system converting kinetic energy into random motions. In order to obtain the surface density, we need to obtain the density profiles of haloes. The first step to obtain this goal is to calculate the initial density profile produced by a primordial fluctuation, $\delta_i(x_i)$, given by Bardeen et al. (1986, hereafter BBKS). Throughout the paper, we adopt the BBKS spectrum and a ΛCDM cosmology with WMAP3 parameters, $\Omega_m = 1 - \Omega_\Lambda = 0.24$, $\Omega_\Lambda = 0.76$, $\Omega_b = 0.043$, and $h = 0.73$, where h is the Hubble constant in units of $100\,\mathrm{km\,s^{-1}\,Mpc^{-1}}$. In reality, the initial density peak is not smooth, but contains many smaller scale positive and negative perturbations that originate in the same Gaussian random field producing the main peak. These secondary perturbations will perturb the motion of the dark matter particles from their otherwise purely radial orbits. Therefore, in order to investigate effects such as tidal torques and non-radial collapse, it is necessary to consider the non-spherical portion of the density distribution. To this aim, the overall initial density profile, evolved linearly to the present day, can be written as

$$\rho(\mathbf{x}) = \rho_0[1 + \delta_0(x)][1 + \epsilon_0(\mathbf{x})], \tag{18}$$

where ρ_0 is the present-day background density, the density excess due to the main halo is $\delta_0(x)$, and is assumed to be spherically symmetric, and $\epsilon_0(\mathbf{x})$ is the density excess caused by the random secondary perturbations (see RG87, DPK09). The magnitude of the extra velocity imparted by secondary perturbation to a typical dark matter particle at the time of turnaround (Eq. [48] of RG87) is

$$|\Delta\mathbf{v}_{\mathrm{rms}}(x, t_{\mathrm{c}}/2)| = F_v(x, t_{\mathrm{c}}/2)\Delta g_0[d(x, t_{\mathrm{c}}/2), x]t_0, \tag{19}$$

where t_{c} is the collapse time, $d(x, t)$ is the comoving displacement, Δg_0 the spatial dependence of acceleration, and F_v the spatial dependence of acceleration (see RG87). The tangential, v_{tan}, and radial, v_{rad}, components of velocity are

$$(\Delta v_{\mathrm{tan}})^2 = \frac{2}{3}|\Delta\mathbf{v}_{\mathrm{rms}}(x)|^2, \quad (\Delta v_{\mathrm{rad}})^2 = \frac{1}{3}|\Delta\mathbf{v}_{\mathrm{rms}}(x)|^2. \tag{20}$$

The collapse starts from the innermost shell, the one adjacent to the core. When the first shell reaches its r_{m}, it collapses and finds its apocenter, r_{a}, and pericenter, r_{p}, within the overall halo potential, $\psi(r)$. It is assumed that the potential changes slowly compared to the dynamical timescales of the shells, so that every shell conserves its adiabatic invariants, the radial and tangential momenta

$$j_\theta(x) = \Delta v_{\mathrm{tan}}\, r_{\mathrm{m}} \tag{21}$$

$$j_r(x) = \int_{r_p}^{r_a} v_{\mathrm{rad}}\, dr \tag{22}$$

throughout the collapse. This is an important assumption in the RG87, Williams et al. (2004), and DPK09 formalism, it is crucial to the computation of dynamics of shell crossing. At r_{m}, the average dark matter particle in the shell acquires its additional random velocity, given by Eq. (19) and Eq. (20).

The radial component of velocity, v_{rad} is given by

$$\frac{dv_r}{dt} = \frac{h^2(r,\nu) + j^2(r,\nu)}{r^3} - G(r) - \mu\frac{dr}{dt} \tag{23}$$

(Peebles 1993; DPK09), where $h(r,\nu)$ is the ordered specific angular momentum generated by tidal torques, $j(r,\nu)$ is the random angular momentum (see RG87), $G(r)$ is the gravitational acceleration, and μ is the coefficient of dynamical friction. In the present paper, we take into account both types of angular momentum: random, j, and ordered, h. As described in RG87, to calculate the ordered angular momentum, one has first to obtain the rms torque, $\tau(r)$, on a mass shell and then calculate the total specific angular momentum, $h(r,\nu)$, acquired during expansion, by integrating the torque over time (R88a, Eq. 35) In order to calculate μ, we recall that, in hierarchical universes, matter is concentrated in lumps, and the lumps into groups and so on, which act as gravitational field generators. One can calculate the stochastic force generated by these field generators and then, following Kandrup (1980), the dynamical friction force per unit mass:

$$\begin{aligned}\mathcal{F} &= -\mu v = -\frac{4.44[Gm_{\mathrm{a}}n_{\mathrm{ac}}]^{1/2}\log\left(1.12N^{2/3}\right)}{N}\frac{v}{a^{3/2}} = \\ &\quad -\beta_o\frac{v}{a^{3/2}}, \end{aligned} \tag{24}$$

where $N = \frac{4\pi}{3} R_{\mathrm{sys}}^3 n_{\mathrm{a}}$, is the total number of field particles, m_{a} and n_{a} are, respectively, the average mass and the number density of the field particles, $n_{\mathrm{ac}} = n_{\mathrm{a}} \times a^3$ is the comoving number of field particles, and a is the expansion parameter, connected to the proper radius of a shell by

$$r(r_i, t) = r_i a(r_i, t). \tag{25}$$

The number and mass of the field generators is calculated using the theory of Gaussian random fields (BBKS86).

The radial distribution of mass within a shell between apocenter and pericenter is not uniform. The density in the radial range dr around r (or equivalently the probability $P(r)dr$ that the particle is in the radial range $r \rightarrow r+dr$) is proportional to the amount of time the particle spends there, (Eq. [53] of RG87):

$$P(r) \ dr = \frac{v_{\mathrm{rad}}^{-1} \ dr}{\int_{r_p}^{r_a} v_{\mathrm{rad}}^{-1} \ dr}. \tag{26}$$

If M_{shell} is the mass of the added shell, then the total mass distribution of the core and shell together is:

$$M_1(r) = M(r) + M_{\mathrm{shell}} \int_{r_p}^{r} P(r')dr'. \tag{27}$$

From this mass function, the new potential $\psi_1(r)$ is calculated. The next mass shell is added and its probability distribution is calculated in the potential $\psi_1(r)$. However, the mass distribution of a newly added shell overlaps with shells that have collapsed earlier; that is, the pericenter of the shell is at a smaller radius than the apocenters of some fraction of the previously added shells. Thus, after adding each new shell, we must recompute the orbits for each shell with which it overlaps. Since the potential does not change violently, the adiabatic invariants of the orbits are conserved. In this case, the adiabatic invariants are the angular momentum j_θ and the radial action j_r. By repeatedly adding shells in this manner, while adjusting the orbits so that the angular momentum and radial action of the orbits are conserved, a self-consistent mass distribution is built up.[8]

The shape of the central density profile is influenced by baryonic collapse: baryons drag dark matter in the so-called adiabatic contraction (AC) steepening the dark matter density slope. Blumenthal et al. (1986) described an approximate iterative analytical model to calculate the effects of AC[9]. More recently, Gnedin et al. (2004) proposed a simple modification of the Blumenthal et al. model, which describes numerical results more accurately. The adiabatic contraction was taken into account by means of Gnedin et al.'s (2004) model. In order to calculate halo surface density, one can fit the density profiles or rotation curves by means of DM profile models or calculating the dark matter column density, as described in the main text of the paper.

---

[8] In other words, the mass particles, once position and velocities are assigned, are allowed to follow the appropriate orbit in the gravitational potential of the previously collapsed matter. As each mass shell is added, those previously added shells with which it overlaps have their orbits adjusted so that the angular momentum j_θ and radial moments j_r integrated from pericenter to apocenter are conserved.

[9] The solutions of their equation are obtained through iterative techniques (Spedicato et al. 2003).

REFERENCES

Adams J. J. 2014, ApJ, 789, 63

Ade P. A. R., Aghanim N., Armitage-Caplan C. et al. 2014, A&A, 571, A16

Astashenok A. V., Del Popolo A. 2012, Class. Quant. Grav., 29, 085014

Babyk Yu. V., Del Popolo A., Vavilova I. B. 2014, Astron. Rep., 58, 587

Bardeen J. M., Bond J. R., Kaiser N., Szalay A. S. 1986, ApJ, 304, 15 (BBKS86)

Blumenthal G. R., Faber S. M., Flores R., Primack J. R. 1986, ApJ, 301, 27

Boyarsky A., Ruchayskiy O., Iakubovskyi D., Macció A. V., Malyshev D. 2009, arXiv: 0911.1774 (B09)

Boyarsky A., Neronov A., Ruchayskiy O., Tkachev I. 2010, Phys. Rev. Lett., 104, 1301 (B10)

Cardone V. F., Del Popolo A. 2012, MNRAS, 427, 3176 (CD12)

Cardone V. F., Tortora C. 2010, MNRAS, 409, 1570 (CT10)

Cardone V. F., Leubner M. P., Del Popolo A. 2011a, MNRAS, 414, 2265

Cardone V. F., Del Popolo A., Tortora C., Napolitano N. R. 2011b, MNRAS, 416, 1822

de Blok W. J. G., Walter F., Brinks E. et al. 2008, AJ, 136, 2648

Del Popolo A. 2002, MNRAS, 336, 81

Del Popolo A. 2007, Astron. Rep., 51, 169

Del Popolo A. 2009, ApJ, 698, 2093

Del Popolo A. 2010, MNRAS, 408, 1808

Del Popolo A. 2011, JCAP, 07, 014

Del Popolo A. 2012a, MNRAS, 424, 38

Del Popolo A. 2012b, MNRAS, 419, 971

Del Popolo A. 2013, AIP Conf., 1548, 2

Del Popolo A. 2014a, IJMPD, 23, No. 3, 1430005

Del Popolo A. 2014b, JCAP, 07, 019

Del Popolo A., Gambera M. 1996, A&A, 308, 373

Del Popolo A., Gambera M. 1997, A&A, 321, 691

Del Popolo A., Hiotelis N. 2014, JCAP, 01, 047

Del Popolo A., Kroupa P. 2009, A&A, 502, 733 (DPK09)

Del Popolo A., Le Delliou M. 2014, JCAP, 12, 051

Del Popolo A., Cardone V. F., Belvedere G. 2013a, MNRAS, 429, 1080

Del Popolo A., Pace F., Lima J. A. S. 2013b, MNRAS, 430, 628

Del Popolo A., Pace F., Lima J. A. S. 2013c, IJMPD, 22, 1350038

Del Popolo A., Pace F., Maydanyuk S. P. et al. 2013d, Phys. Rev. D, 87, 043527

Del Popolo A., Lima J. A. S., Fabris J. C., Rodrigues D. C. 2014, JCAP, 04, 021

Donato F., Gentile G., Salucci P., Frigerio M. C. 2009, MNRAS, 397, 1169 (D09)

Ferreras I., Sakellariadou M., Yusaf M. F. 2008, Phys. Rev. Lett., 100, 1302

Gentile G., Famaey B., Zhao H., Salucci P. 2009, Nature, 461, 627 (G09)

Gnedin O. Y., Kravtsov A. V., Klypin A. A., Nagai D. 2004, ApJ, 616, 16

Governato F., Brook C., Mayer L. et al. 2010, Nature, 463, 203

Gunn J. E., Gott J. R. 1972, ApJ, 176, 1

Hashim N., De Laurentis M., Abidin Z. Z., Salucci P., 2014, arXiv: 1407.0379

Hayashi E., Navarro J. F., Power C. et al. 2004, MNRAS, 355, 794

Hiotelis N., Del Popolo A. 2006, Ap&SS, 301, 67

Hiotelis N., Del Popolo A. 2013, MNRAS, 436, 163

Iocco F., Pato M., Bertone G. 2015, Phys. Rev. D, 92, 084046

Kandrup H. E. 1980, Phys. Rep., 63, 1

Klypin A., Kravtsov A. V., Valenzuela O., Prada F. 1999, ApJ, 522, 82

Kormendy J., Freeman K. C. 2004, IAU Symp., ASP, 220, 377 (KF04)

Kuzio de Naray R., McGaugh S. S., de Blok W. J. G. 2008, ApJ, 676, 920

Mamon G. A., Lokas E. L. 2005, MNRAS, 362, 95

Milgrom M. 1983a, ApJ, 270, 365

Milgrom M. 1983b, ApJ, 270, 371

Milgrom M. 2009, MNRAS, 398, 1023

Moffat J. W., Toth V. T. 2015, Phys. Rev. D, 91, 043004

Moore B. 1994, Nature, 370, 629

Napolitano N. R., Romanowsky A. J., Tortora C. 2010, MNRAS, 405, 2351 (NRT10)

Oh S.-H., Brook C., Governato F. et al. 2010, AJ, 142, 24

Oh S,-H., de Blok W. J. G., Brinks E. et al. 2011, AJ, 141, 193

Pace F., Batista R. C. Del Popolo A. 2014, MNRAS, 445, 648

Peebles P. J. E. 1993, *Principles of Physical Cosmology*, Princeton University Press

Randriamampandry T., Carignan C. 2014, MNRAS, 439, 2132

Ryden B. S. 1988a, ApJ, 329, 589 (R88a)

Ryden B. S. 1988b, ApJ, 333, 78 (R88b)

Ryden B. S., Gunn J. E. 1987, ApJ, 318, 15 (RG87)

Saburova A., Del Popolo A. 2014, MNRAS, 445, 3512 (SD14)

Sanchez-Salcedo F. J., Reyes-Iturbide J., Hernandez X. 2006, MNRAS, 370, 1829

Sikivie P., Tkachev I. I., Wang Y. 1997, Phys. Rev. D., 56, 1863

Spedicato E., Bodon E., Del Popolo A., Mahdavi-Amiri N. 2003, 4OR, Vol. 1, Issue 1, 51

Stadel J., Potter D., Moore B. et al. 2009, MNRAS, 398, 21

Weinberg S. 1989, Rev. Mod. Phys., 61, 1

Williams L. L. R., Babul A., Dalcanton J. J. 2004, ApJ, 604, 18